Clim Dyn
DOI 10.1007/s00382-017-3924-2

# Local onset and demise of the Indian summer monsoon

**Vasubandhu Misra**[1,2,3] · **Amit Bhardwaj**[1,3] · **Akhilesh Mishra**[1,4]

Received: 24 July 2017 / Accepted: 19 September 2017


**Abstract** This paper introduces an objective definition of local onset and demise of the Indian summer monsoon (ISM) at the native grid of the Indian Meteorological Department's rainfall analysis based on more than 100 years of rain gauge observations. The variability of the local onset/demise of the ISM is shown to be closely associated with the All India averaged rainfall onset/demise. This association is consistent with the corresponding evolution of the slow large-scale reversals of upper air and ocean variables that raise the hope of predictability of local onset and demise of the ISM. The local onset/demise of the ISM also show robust internannual variations associated with El Nino and the Southern Oscillation and Indian Ocean dipole mode. It is also shown that the early monsoon rains over northeast India has a predictive potential for the following seasonal anomalies of rainfall and seasonal length of the monsoon over rest of India.

**Keyword** Indian monsoon · ENSO · Onset of monsoon

✉ Vasubandhu Misra
vmisra@fsu.edu

[1] Center for Ocean-Atmospheric Prediction Studies, Florida State University, Tallahassee, FL, USA

[2] Department of Earth, Ocean and Atmospheric Science, Florida State University, Tallahassee, FL, USA

[3] Florida Climate Institute, Florida State University, Tallahassee, FL, USA

[4] Amity Center for Ocean–Atmosphere Science and Technology, Amity University, Jaipur, Rajasthan, India

## 1 Introduction

The Indian Summer Monsoon (ISM) onset and demise is a dramatic change in the hydroclimate of the region that brings relief from the repressive heat of the pre-monsoon period while also replenishing the terrestrial freshwater supply to meet the needs of area inhabitants. The variability of the ISM's seasonal evolution is also closely tied to the economy of the region (Rosenzweig and Binswanger 1993; Gadgil and Gadgil 2006; Gine et al. 2008). The IMD has been ascertaining the date of the Monsoon onset of Kerala (in the southwest corner of India; MoK) systematically for several decades (Pai and Rajeevan 2007). This monitoring of the onset has evolved from being based simply on rainfall (Ananthakrishnan et al. 1967, 1968; Sperber and Annamalai 2014; Noska and Misra 2016) to a more comprehensive outlook of wind field, outgoing longwave radiation and rainfall (Joseph et al. 2006; Pai and Rajeevan 2007; Wang et al. 2009), moisture flux convergence (Fasullo and Webster 2003), and precipitable water (Zeng and Lu 2004; Lu et al. 2009).

Despite this expansion of measures by which the onset of the ISM is now defined, we argue that continuing to base it on the MoK or other specific sub-regions of the ISM is inadequate and often untimely, especially for rural agrarian households spread across the country. For example, Bansod et al. (1991) found that the advance of the ISM after MoK is rather pulsatory and that onset in the southwest corner of India is only somewhat tied to onset across the rest of India. In fact, it can take anywhere from days to weeks for the ISM to reach other parts of India. Thus, while the MoK is currently the earliest indication of the system's onset, it does not initiate a clear timeline for onset of the ISM elsewhere in the country. So, in regions such as India where agricultural production is largely rain-fed and widespread formal insurance

Published online: 09 October 2017

markets to protect farmers are lacking, there is a continuous struggle to balance between maximizing profits and lowering risk (Walker and Ryan 1990; Gine et al. 2008). Moron and Robertson (2014) defined a local onset for the ISM based on agronomic necessity that ensured sufficient soil moisture in the subsequent days after the local onset for germination of the planted seeds. This was a threshold-based definition such that at least a 5-day wet sequence (of $\geq 1\,\mathrm{mmday}^{-1}$) followed after the diagnosis of the local onset and without being followed further by a desiccating 10-day dry spell in the 30 days following the first rains. Such restrictive definitions serve very well as a diagnostic tool but are more difficult to use as a real-time monitoring tool. Similarly, a grid based rainfall onset index for the Asian monsoon was proposed in Wang and LinHo (2002). This was yet again threshold based definition, contrasting rainfall pentads with the January (winter) mean precipitation (relative pentad mean rain rate). Wang and LinHo (2002) suggest a pre-determined threshold of $5\,\mathrm{mmday}^{-1}$ to the relative pentad mean rain rate. The onset date in Wang and LinHo (2002) is detected as the first pentad of the season that exceeds this threshold. However, this methodology is susceptible to false onsets, when transient weather systems produce copious rainfall that exceed this threshold.

In more recent studies, (Noska and Misra 2016; Misra et al. 2017) showed that the onset and demise of the ISM based on the All India averaged Rainfall (AIR) has robust relationships with the large-scale changes in ocean and atmospheric circulation and land–ocean thermal gradients. Many of these large-scale changes are, in turn, associated with important energy transformations (Krishnamurti et al. 1981, 2017) and instabilities (Tomas and Webster 1997; Krishnakumar and Lau 1998; Goswami and Xavier 2005). While it is argued that onset and demise of the ISM based on AIR would be a logical assumption because of its intimate relationship to large-scale dynamical and thermodynamical changes, the practical significance of this approach is rather limited because of the non-representative nature of the area-average. In this paper, we propose a definition for local onset and demise of the ISM based solely on rainfall. This new definition allows us to leverage a widely used long record of rain gauge observations of the ISM (Pai et al. 2014a, b) to understand low frequency variations of the propagation of isochrones of onset and demise and avoid the use of model biased upper air variables from reanalysis or bias in satellite retrievals (Gadgil et al. 1992; Goswami and Sengupta 2003; Misra et al. 2012; Shah and Mishra 2014). Furthermore, the relatively scarce availability of radiosonde observations in time and space impedes their use for historical analysis of onset and demise of the ISM (Waliser et al. 1999). The proposed definition also offers the flexibility to adapt to desired spatial scales based on the needs of the users.

Our attempt at honing on a local definition of onset and demise of the ISM is timely given the growing awareness of a need to target global forecasts with a regional or local focus in order to avert or ameliorate the impact of natural weather and climate disasters in the developing world (Webster 2013; Lucas-Picher et al. 2011).

## 2 Methodology and datasets

We make use of the daily rainfall analysis based on rain gauge measurements available from the Indian Meteorological Department at $0.25° \times 0.25°$ grid interval (Pai et al. 2014a, b). The onset and demise of the ISM follows from Noska and Misra (2016), who define onset (demise) as the first day after the minimum (maximum) in daily cumulative anomaly of AIR is reached in the year. The daily cumulative anomaly $C'_m(i)$ of AIR for day i of year m is computed as:

$$C'_m(i) = \sum_{n=1}^{i} \left[ A_m(n) - \overline{\overline{C}} \right] \tag{1}$$

where,

$$\overline{\overline{C}} = \frac{1}{MN} \sum_{m=1}^{M} \sum_{n=1}^{N} A(m,n) \tag{2}$$

$A_m(n)$ is the daily AIR for day n of year m, and $\overline{\overline{C}}$ is the climatology of the annual mean of AIR over N (=365/366) days for M years.

To define the local onset and demise at every grid point over the domain we first compute the climatological local onset ($\overline{o(i)}_x$) and demise ($\overline{d(i)}_x$) from the daily cumulative anomaly ($cl'_x(i)$) of the daily climatology of rain at the grid point in the same way as for the AIR (but this local definition can be potentially scaled to any spatial discretization that suits user needs):

$$cl'_x(i) = \sum_{n=1}^{i} \left[ \bar{r}_x(n) - \overline{\overline{c_x}} \right] \tag{3}$$

where, $\bar{r}_x$ is the climatological rain at grid point x for day n and $\overline{\overline{c_x}}$ is annual mean climatology of rain at grid point x:

$$\overline{\overline{c_x}} = \frac{1}{MN} \sum_{m=1}^{M} \sum_{n=1}^{N} r(m,n)_x \tag{4}$$

Similarly, we define the climatological onset ($\overline{O(i)}_x$) and demise ($\overline{D(i)}_x$) from the daily cumulative anomaly of the daily climatological AIR. We then compute the difference ($b_x$) between the climatological local ($\overline{o(j)}_x$) and climatological AIR onset ($O(i)$) as:

$$b_x = \overline{o(j)_x} - \overline{O(i)} \quad (5)$$

and similarly, the difference ($d_x$) between the climatological local ($\overline{d(j)_x}$) and AIR demise ($D(i)$) as:

$$d_x = \overline{d(j)_x} - \overline{D(i)} \quad (6)$$

The climatological departures of local with AIR-based onset/demise over the 104-year period of the dataset gives a robust estimate of the phase lag (in days), with the transients being averaged out. We then define local onset ($lc_m(i)_x$) and demise ($ld_m(i)_x$) for a given year $m$ and grid point $x$ from the daily cumulative anomaly for the year $m$ by finding conservatively (the nearest) minimum and maximum near the immediate vicinity of ($O_m(i) \pm kb_x$) and ($D_m(i) \pm pd_x$), where, $k = \left(1 + q\sigma_{b_x}\right)$ and $p = \left(1 + r\sigma_{b_x}\right)\sigma_{b_x}$, $\sigma_{d_x}$, are the standard deviations of $b_x$ and $d_x$, $q$ and $r$ are fractions that are incrementally increased from zero. This is a reasonable strategy designed to avoid the likelihood of the diagnosis of false onset (demise) characterized by prolonged dry (wet) spell as it finds the inflexion point closest to the climatological departure from onset (demise) of AIR.

In addition to the rainfall dataset the upper air variables are analyzed from the centennial reanalysis of the European Center for Medium-Range Weather Forecasting (ERA-20C; Poli et al. 2016). This dataset is available at daily interval at T159 spectral truncation (~ 125 km) resolution and overlaps with the time period of the IMD rainfall analysis. Furthermore, we also make use of the upper ocean variables from the Climate Forecast System Reanalysis (CFSR; Saha et al. 2010), which is available at 0.5° grid spacing from 1979 to 2010. The statistical significance of the correlations follow

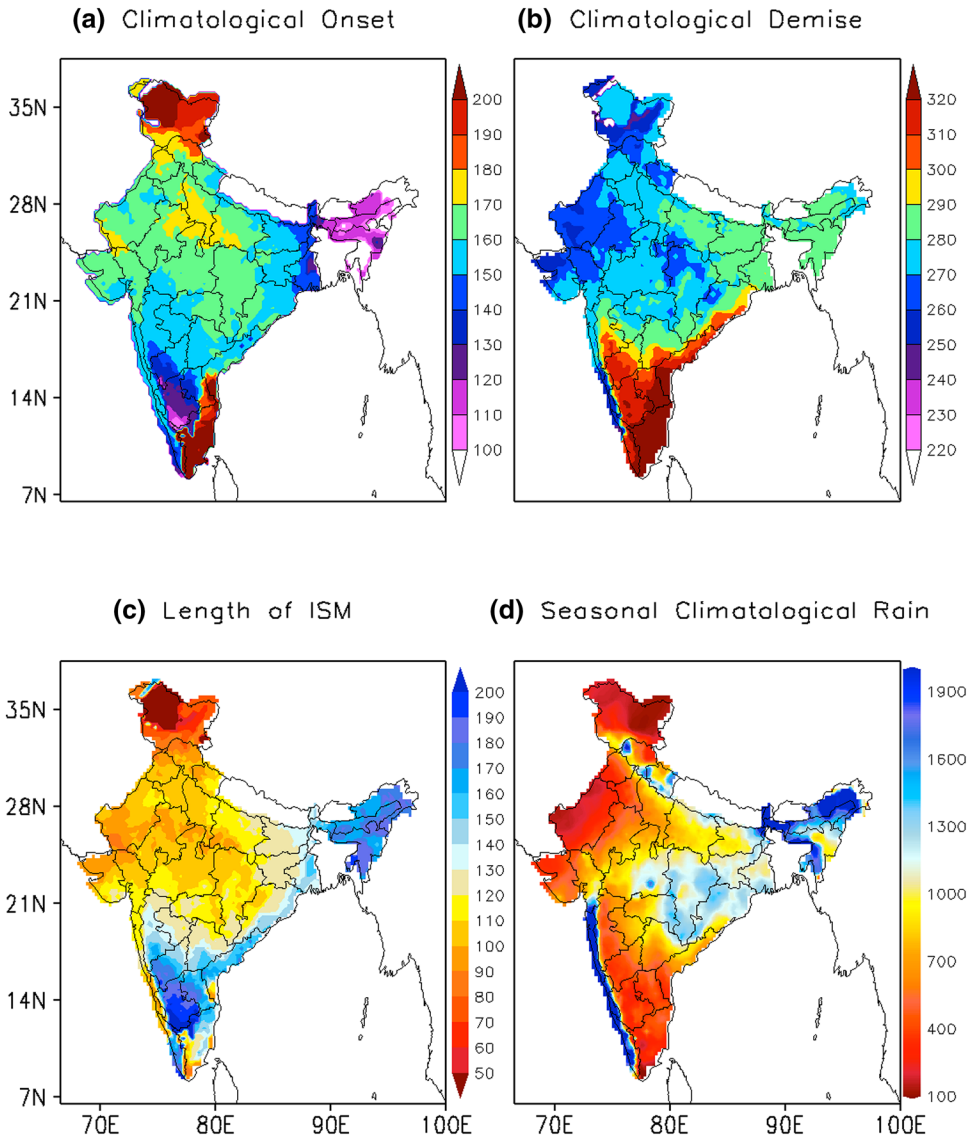


**Fig. 1** The climatological **a** onset and **b** demise date (in Julian days), and **c** length (in days) of the Indian Summer Monsoon (ISM) defined at every grid point of the Indian Meteorological Department (IMD) gridded rainfall dataset at 0.25° grid interval. **d** The climatological seasonal mean rainfall (mm), accumulated between the climatological local onset and demise date of the ISM at each grid point

the non-parametric test of bootstrapping technique (Efron and Tibshirani 1993).

## 3 Results

### 3.1 Climatological local onset and demise

The climatological local onset ($\overline{o(i)}_x$) and demise ($\overline{d(i)}_x$) of the ISM are shown in Fig. 1a, b, respectively. In general, the progression of the local onset of the ISM in Fig. 1a follows the typical isochrone progression of the ISM from the southwest corner across to the northwest regions of India. However, the southeastern part of India (Tamil Nadu) and over northern tip of India (northwestern part of Jammu and Kashmir) experience a very delayed onset of the ISM (Fig. 1a), as these regions climatologically receive far less summer season rainfall than other parts of the country (Fig. 1d).

Portions of southern Karnataka have very early onset of the rains, even before the onset over Kerala (Fig. 2a). Early onset in the southern Deccan plateau is a result of spring season rains in the region, which are less than 5mmday$^{-1}$ and happen much before the prevailing low-level southwesterly flow (not shown). These are often referred as pre-monsoon showers. However, they transition to the summer rains rather smoothly (e.g. Fig. 2a), which forces our algorithm to detect the onset of the ISM very early in this part of India. For the sake of comparison, we look at the diagnosis of the climatological onset and demise over Mysore in southern Karnataka (12.2°N and 76.6°E; Fig. 2a) and Bhopal in Madhya Pradesh (23.3°N and 77.4°E; Fig. 2b) to show the uniformity in our definition of local onset and demise of ISM. Any distinction between pre-monsoon and monsoon rains in the southern Deccan plateau would have to be realized by using other criterion (e.g. based on wind and moisture variables), which would potentially introduce complexity and further uncertainty to the analysis. In addition, we find that variations of the onset of these pre-monsoon rains over the southern Deccan plateau detected by the algorithm has high correlations with the corresponding local length of the monsoon season and with those of the AIR based length of the season variations (shown later). This essentially suggests that the pre-monsoon rains in the southern Deccan plateau could be a necessary precursor for the monsoon rains in the southern Deccan plateau.

Likewise, northeastern parts of India (NI; consisting of Assam, Arunachal Pradesh, Manipur, Meghalaya, Mizoram,

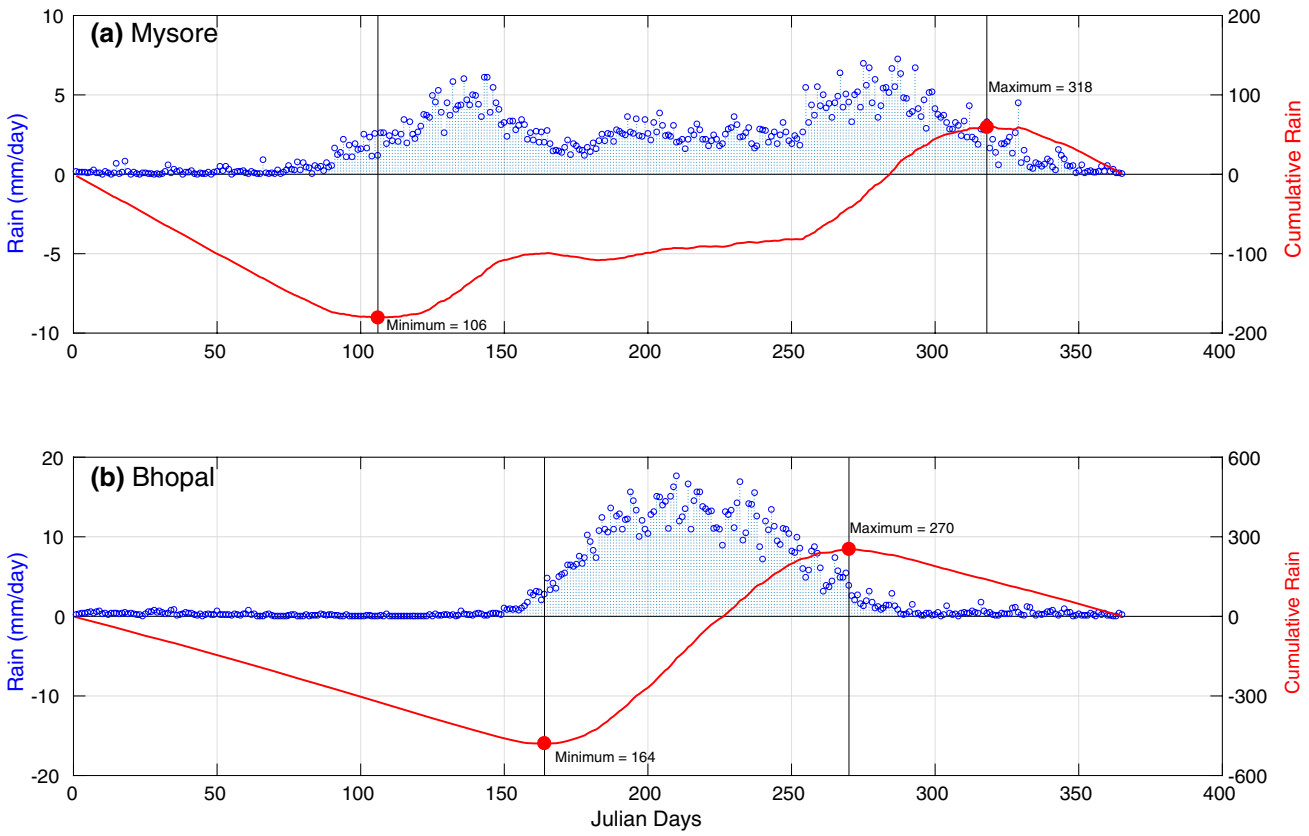


**Fig. 2** Daily climatological rain rate (in blue) over **a** Mysore in southern Karnataka (12.2°N and 76.6°E) and **b** Bhopal in Madhya Pradesh (23.3°N and 77.4°E). The corresponding daily cumulative anomaly of rainfall (in red) and the diagnosed onset and demise dates (in Julian day) are indicated by the minimum and maximum in the curve respectively

Sikkim, and Tripura) also experience very early onset dates (Fig. 1a). Similarly, the demise of the ISM in Fig. 1b follows from the northwestern parts of India and the southwestern coast, through the Indo-Gangetic plains and NI, and lastly out of the southern Deccan plateau. The delayed demise over the southeastern coast of India is a result of the prevailing rains from the northeast winter monsoon.

The length of the ISM season (Fig. 1c) is longest over south-central Karnataka and NI, consistent with the diagnosis of early onset (Fig. 1a) over these regions. But the climatological seasonal accumulation of rainfall of the ISM (Fig. 1d) suggests that the highest accumulation is along the western coast and NI, followed by that over central, eastern, and northern India. This would imply that the climatological daily rain rate over south-central Karnataka is relatively weak such that the seasonal accumulation is less despite the long length of the rainy season. On the other hand, NI is one the highest rainfall receiving regions on the planet with an

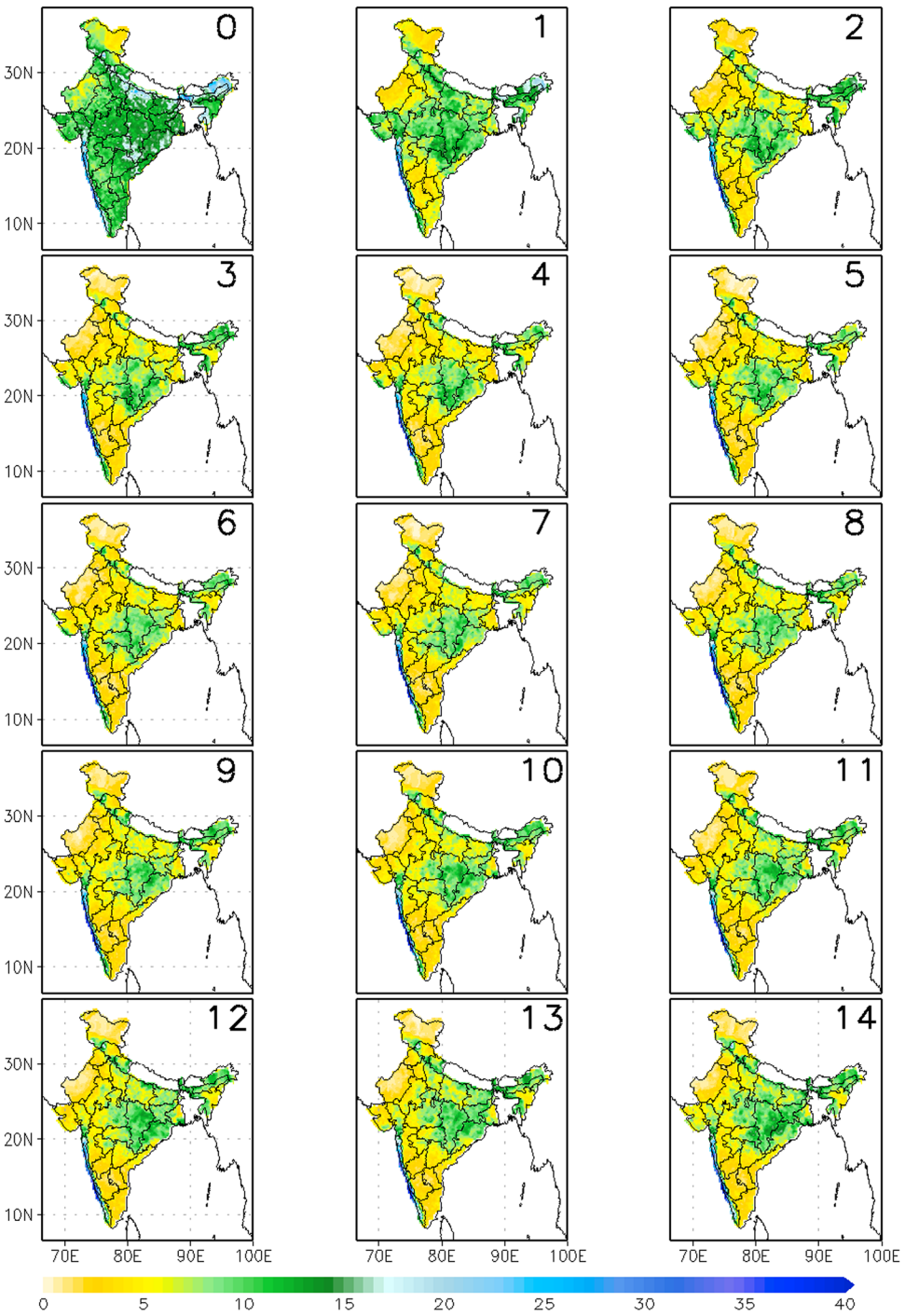


**Fig. 3** The climatological daily rainfall (mmday$^{-1}$) at time of time of onset (0) and in the subsequent 14 days

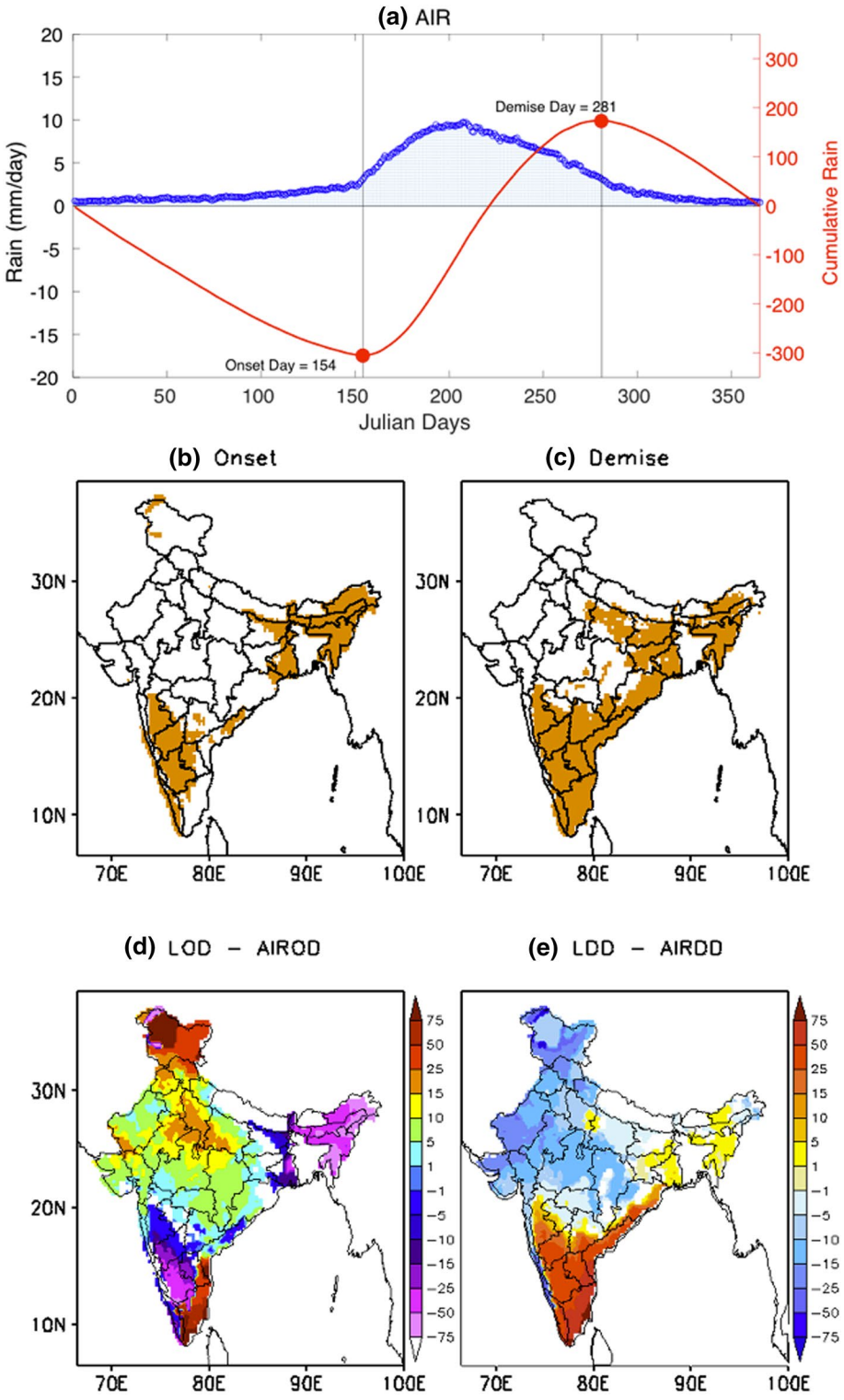


**Fig. 4** **a** Time series of daily climatology of the All India averaged Rainfall (AIR; blue line) and the corresponding cumulative daily anomaly curve (red line) with the onset (AIROD) and demise (AIRDD) dates marked in Julian days. The regions where climatological local onset (marked in brown) has occurred on the date of **b** AIROD and **c** the regions where climatological local demise has yet to occur on the date of AIRDD (marked in brown). The difference (in days) between climatological Julian days of **d** local onset (LOD) and AIROD and **e** local demise (LDD) and AIRDD

annual average of 2068 mm (Jain et al. 2013). It should be noted that the mean daily climatological rainfall for the 15 days subsequent to the diagnosis of the local onset is well over 1 mmday$^{-1}$ (Fig. 3).

### 3.2 Relation of climatological local onset and demise with AIR onset and demise

In Fig. 4a the climatological onset and demise of the AIR are identified with a Julian day of 154 and 281 from the daily

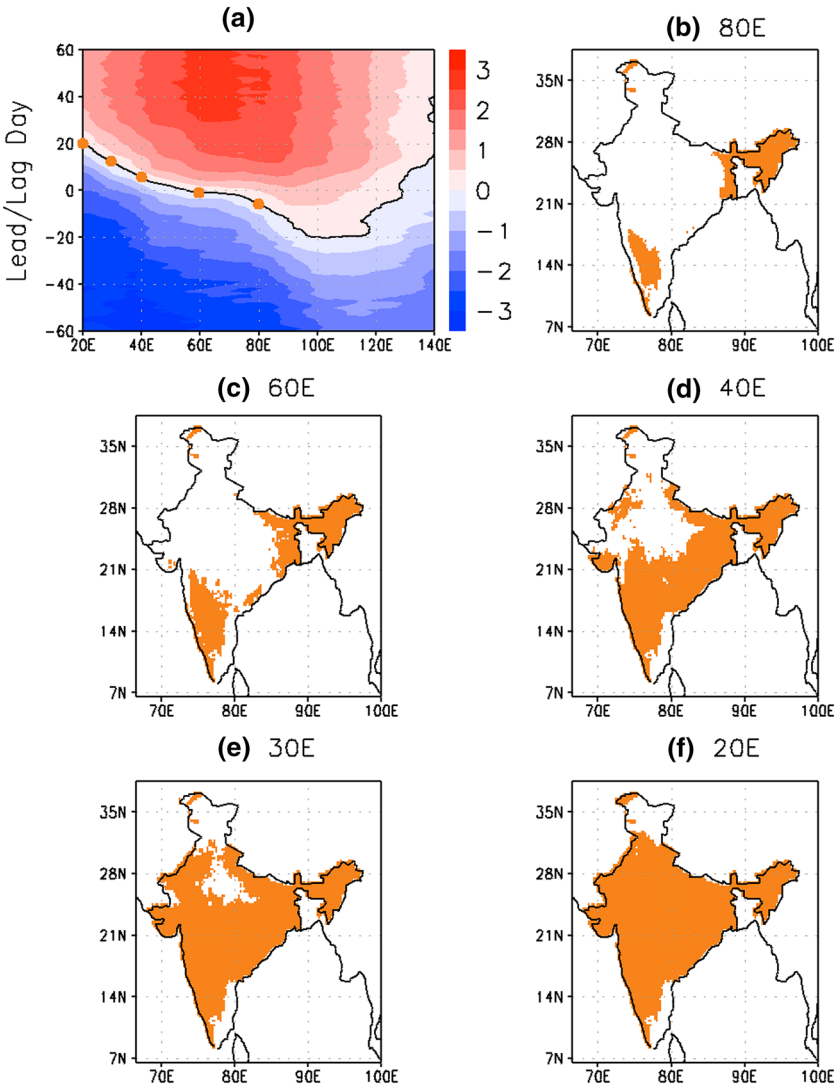


**Fig. 5** **a** The climatological daily zonal progression of the meridional temperature gradient between 5°N and 25°N at 300 hPa as function of lead/lag time with respect to the onset date of AIR. The climatological progression of the local onset date of the ISM shown at times when the meridional temperature gradient reverses as indicated by the filled brown circles over the zero-contour line highlighted in (a) crossing at **b** 80°E, **c** 60°E, **d** 40°E, **e** 30°E, and **f** 20°E. The brown shading in panels **b**–**f** indicate points where local onset has occurred

climatological AIR, respectively. The regions that manifest with climatological local onset of the ISM corresponding to the climatological onset date of AIR are indicated in Fig. 4b. As Fig. 4b illustrates, climatologically the AIR onset occurs over the southwestern coast of India, parts of southern and eastern Deccan plateau, and over NI. Similarly, at the time of the climatological demise of AIR, northwestern and parts of central India also undergo the demise of the ISM; however, NI, the Deccan plateau, and the eastern coast of India continue to be under the influence ISM (Fig. 4c). The differences in the climatological local and AIR onset date shown in Fig. 4d indicates that the southwestern coast of Kerala, parts of southern Deccan plateau, and a majority of northeastern states of India experience their onset of the ISM nearly 25 to 50 days prior to the AIR onset, while central and northwestern India experience their onset 5 to 15 days after the AIR onset. Similarly, the corresponding differences of the demise dates shown in Fig. 4e reveal the earlier local demise of the ISM along the Konkan coast, in northwestern India, and in parts of central India by 10 to 25 days relative to the AIR demise, and a later local demise in the Deccan plateau, along southwestern coast of Kerala, and over Tamil Nadu by about 15–50 days.

### 3.3 Large-scale reversals and progression of the ISM

The ISM has a robust seasonal signal with a clear reversal of the large-scale temperature gradient, especially at the upper levels where the Tibetan plateau serves as an elevated heat source (Yanai et al. 1992; Webster et al. 1998; Noska and Misra 2016). In Fig. 5 we see the progression of the climatological local onset with the reversal of the temperature gradient at 300 hPa. For example, when the temperature reverses at 80ºE (i.e., zero line of the temperature gradient reaches 80ºE in Fig. 5a) the local onset is only over eastern Deccan plateau (Fig. 5b). But as the reversal of the temperature gradient progresses westward, the local onset of the ISM also progresses across India (Fig. 5b-h). Similarly, the demise

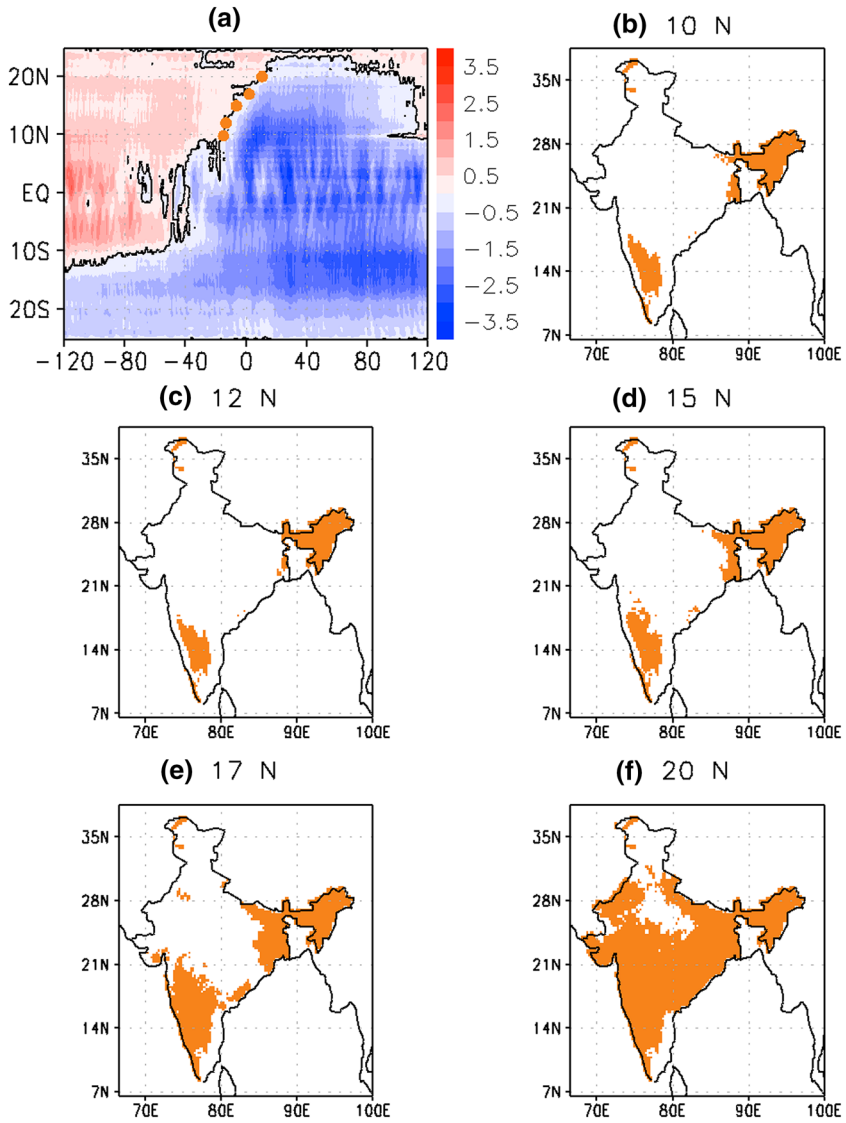


**Fig. 6** The climatological daily meridional progression of the zonally averaged meridional upper ocean (vertically integrated from surface to 105 m below surface) transport as a function of lead/lag with respect to the onset date of AIR. The climatological progression of the local onset date of the ISM shown at times when the meridional ocean heat transport reverses as indicated by the filled brown circles on the zero contour line highlighted in **a** crossing at **b** 10°N, **c** 12°N, **d** 15°N, e 17°N, and **f** 20°N. The brown shading in panels **b–f** indicate points where local onset has occurred

of the ISM entails a withdrawal of the local demise from the northwestern corner of India through the NI and central parts of India (not shown). There are however some recent studies that contest these mechanisms of onset of the ISM by noting in their model simulations that the Tibetan Plateau serves to preserve the moist static energy and the meridional differential of latent heating produced governs the onset of the ISM (Chakraborty et al. 2006; Boos and Kuang 2010, 2013; Ashfaq et al. 2016). In contrast, other studies suggest that moist symmetric instability is triggered by the reversal of the large-scale temperature gradient, which triggers the onset of the ISM (Tomas and Webster 1997; Krishnakumar and Lau 1998; Goswami and Xavier 2005). As these studies suggest, the mechanical and thermal effects of orography as drivers of ISM and trigger for onset of ISM is yet to be clearly discerned.

Similarly, the northward progression of the southward upper ocean heat transport in the tropical Indian Ocean (Wyrtki 1973; Loschnigg and Webster 2000; Webster 2000; Noska and Misra 2016) involves the progression of the onset of the ISM from the southwest and northeast parts to rest of India (Fig. 6). Likewise, the southward expansion of the northward ocean heat transport in the Indian Ocean coincides with a similar withdrawal of the ISM rainfall from the northwest to the southeast parts of India (not shown). The sequential progression of the isochrones of local onset/demise with the seasonal evolution of the large-scale changes in upper air and ocean variables raise the hope for predictability at medium range and seasonal time scales of the onset of the ISM. In fact, this is already being attempted for the MoK (Alessandri et al. 2015; Joseph et al. 2015).

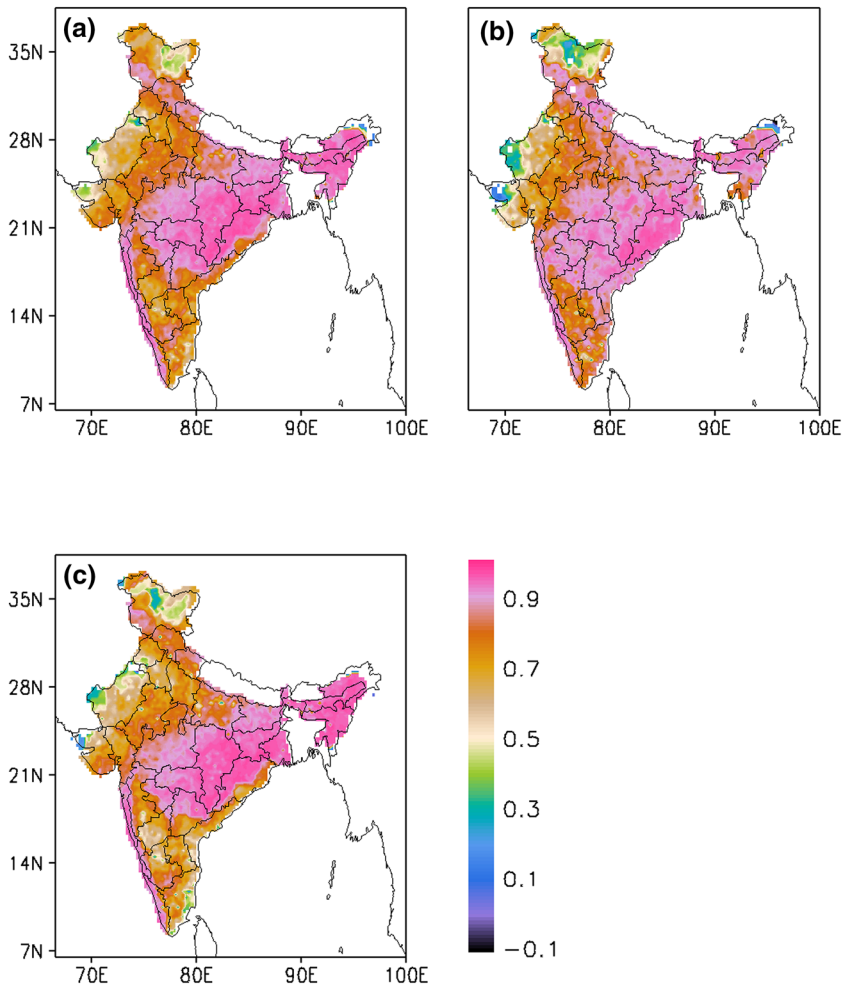


**Fig. 7** The correlation between **a** length of ISM based on AIR index with length of ISM computed at every grid point (local length), **b** onset date based on AIR with local onset date and **c** demise date based on AIR with local demise date variations. All correlations significant at 95% confidence interval according to bootstrap method are shaded

### 3.4 Interannual variations

The contemporaneous correlations of the seasonal mean anomalies of the length of ISM based on the AIR index and with the corresponding length at individual grid points reveal that the two are strongly related over the western coast, central India, and NI (Fig. 7a). They are least correlated over the northwestern parts of India (e.g. Rajasthan), over Jammu and Kashmir, and over southeastern India including parts of Karnataka, Tamil Nadu, and Andhra Pradesh (Fig. 7a). A similar picture emerges for correlations of the onset (Fig. 7b) and demise dates (Fig. 7c). But these large coherent patterns of correlation between local and AIR based indices are consistent with the associated large-scale changes in upper air and ocean variables discussed earlier. For example, Noska and Misra (2016) showed that AIR based onset and demise evolved with large scale atmospheric and ocean circulations in the Indian Ocean region.

The linear correlations of the June–July–August (JJA) Nino3.4 sea surface temperature (SST) seasonal anomalies with local onset (Fig. 8a) and demise (Fig. 8b) of the ISM reveal a statistically significant but albeit relatively weak relationship. These figures show that the warm (cold) phase of the JJA El Niño/Southern Oscillation (ENSO) SST anomalies is likely associated with later (early) onset and/or early (later) demise of the ISM. This is also consistent with the association of the warm (cold) phase of JJA ENSO SST anomalies with the likelihood of shorter (longer) wet season length of the ISM (with slightly stronger correlations than Fig. 3a, b) in large portions of India (Fig. 8c). These teleconnections with ENSO on the onset, demise, and length of the ISM season translate to corresponding associated linear changes in the accumulated seasonal anomalies of rainfall across India (Fig. 8d), although the correlations are less uniform than in the other panels (Fig. 8a–c). Misra et al. (2017) allude to non-canonical relations between length and seasonal rainfall anomalies of the ISM as a result of the ENSO transition from one phase to another that has an opposite bearing on onset date and demise date variations of the ISM. Such seasons can

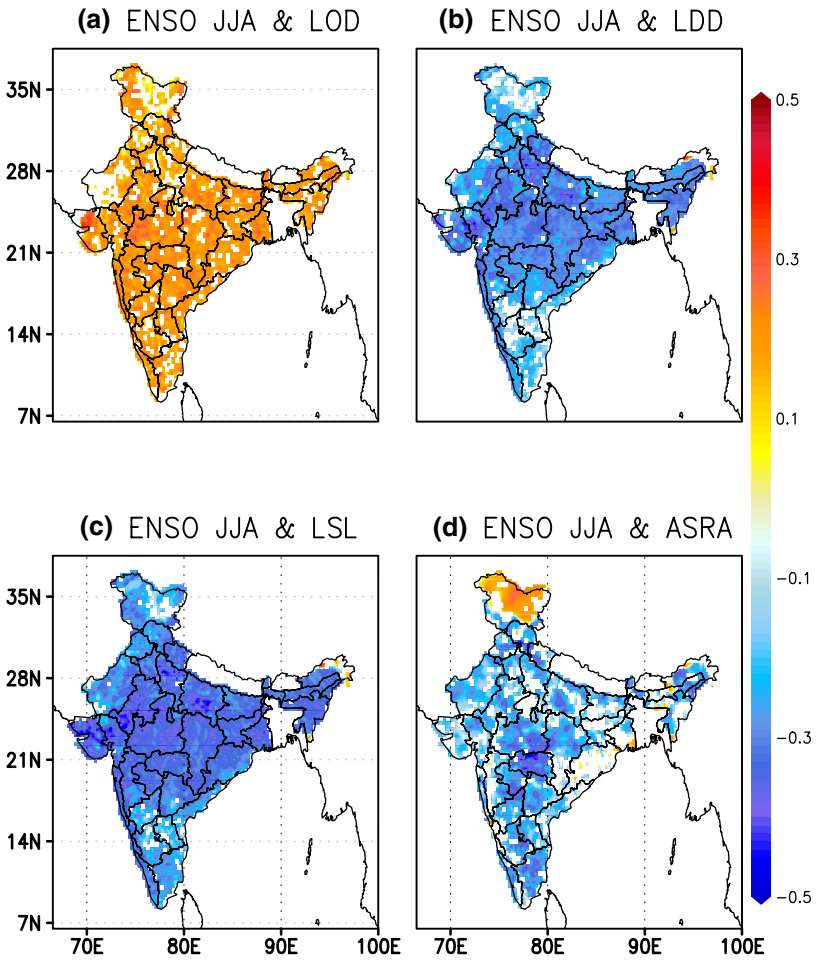


**Fig. 8** The correlation of June-July-August (JJA) seasonal mean Nino3.4 (ENSO) SST anomalies with local **a** onset date (LOD), **b** demise date (LDD), **c** length (LSL), and **d** accumulated seasonal rainfall anomalies (ASRA) of the India Summer Monsoon (ISM) season. All correlations significant at 95% confidence interval according to bootstrap method are shaded

lead to long (short) seasons of ISM with less (more) seasonal rainfall anomalies, which could explain some of the differences in the spatial distribution of the correlations between Fig. 8c, d.

The correlations of the Indian Ocean Dipole (IOD index; IOD is defined as the difference in the seasonal September-October-November mean SST over the western Indian Ocean (50°E–70°E and 10°S and 10°N) and eastern Indian Ocean (90°E–110ºE and 10°S and 0°) with the evolution of the ISM (Fig. 9) reveal that it has an insignificant influence on the local onset (Fig. 9a). That said, the IOD has some significant association with the length of the ISM season (Fig. 9c) based on its relationship with the local demise date (Fig. 9b). A positive (negative) IOD index reveals that it leads to an early (later) demise (Fig. 9b) and shorter (longer) length of the ISM across India (Fig. 9c). However, positive (negative) IOD is associated with more (less) anomalous seasonal rain over central (Madhya Pradesh) and northern (Uttar Pradesh) India. A comparison of Fig. 9c, d suggests that the IOD influences the probability density function of the daily rainfall over these regions, and that despite shortening (lengthening) the season (Fig. 9d) it is associated with a simultaneous increase (decrease) of seasonal rainfall over central and northern India. And over south-central India (e.g. Maharashtra and Karnataka), the positive (negative) IOD variations are associated with shortened (lengthened) ISM season and anomalously less (more) seasonal rainfall.

We therefore further explore the role of the onset date variations of the ISM over NI, given its relatively early onset (Fig. 1a) and the spatially coherent, robust association with corresponding variations of AIR onset (Fig. 7a). It is quite apparent that early (later) onset of the ISM over NI is very strongly associated with early (later) onset (Fig. 10a) and longer (shorter) length (Fig. 10c) of ISM over rest of India. As a consequence, early (later) onset of ISM over NI is associated with more (less) anomalous seasonal rain over eastern and central India (Fig. 10d). However, the relationship of onset of ISM over NI with demise over rest of India is very weak (Fig. 10b). This diagnosed association between variations in the onset of the ISM over NI and the rest of India can best be explained by the corresponding modulation of

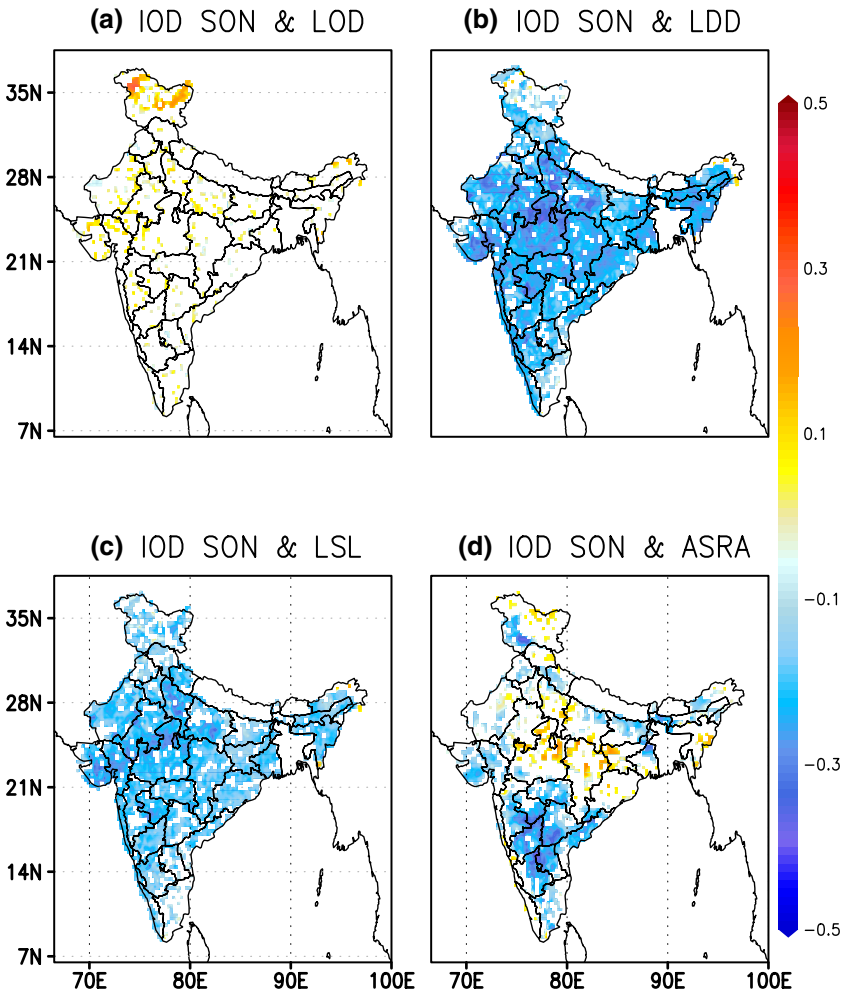


**Fig. 9** The correlation of the September-October-November (SON) Indian Ocean Dipole (IOD) mode index seasonal mean anomalies with local **a** onset date (LOD), **b** demise date (LDD), **c** length (LSL), and **d** accumulated seasonal rainfall anomalies (ASRA) of the India Summer Monsoon (ISM) season. All correlations significant at 95% confidence interval according to bootstrap method are shaded

the low level (850 hPa) southwesterly flow (Fig. 11). Figure 11a suggests that the anomalous early (later) onset of the rains in the NI is associated with enhanced (weakened) seasonal climatological JJA cross-equatorial southwesterly flow into the monsoon trough residing over the Bay of Bengal and central India (Fig. 11b). The anomalous flow configuration associated with anomalous onset of the monsoon rains over NI, as shown in Fig. 11, could lead to zonal mean flow accelerations leading to increased likelihood for onset vortex and monsoon depressions from barotropic instability (Krishnamurti et al. 1981; Lindzen et al. 1983). It may be noted that the correlations in Fig. 5d are stronger in the eastern part of the subcontinent and therefore complimentary to the teleconnections shown in Figs. 3d and 4d. This raises the importance of monitoring the onset of ISM over NI as an additional source of ISM seasonal rainfall predictability.

## 4 Discussion and conclusions

The flexibility of this local definition to adjust to any given spatial scales is quite apparent from its formulation. We have defined in this paper over the native grid of the IMD rainfall analysis. But one could define it similarly at the scale of a province, meteorological division, or conforming to any other boundary of choice of the user. A local definition is however, important for practical applications of understanding and anticipating the ISM evolution from its early onset recognized over NI and Kerala.

While this is purely an observational study, the close association of local onset/demise with the AIR based onset/demise raises hope for the predictability of the local onset and demise of the ISM. The evolution of the large-scale upper air temperature reversal and upper ocean heat transport with the local onset/demise of the ISM is not coincidental but part of a coherent evolution. Therefore, this association with slowly evolving large-scale variations could be exploited by numerical models to develop

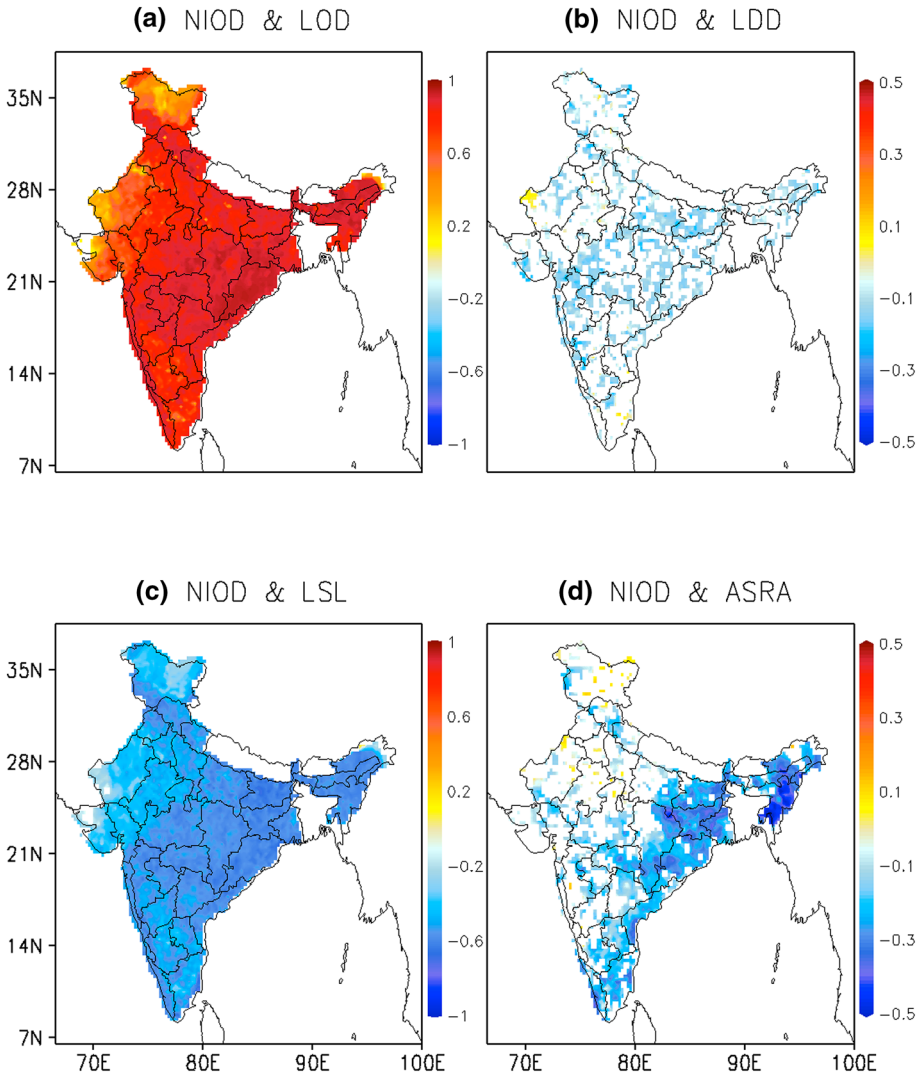


**Fig. 10** The correlation of the area averaged onset date over northeast India (NIOD) with corresponding local **a** onset dates (LOD), **b** demise dates (LDD), **c** seasonal length (LSL), and **d** seasonal rainfall anomalies (ASRA), and **d** demise dates (LDD) of the India Summer Monsoon (ISM). All correlations significant at 95% confidence interval according to bootstrap method are shaded

targeted prediction of the local onset/demise of ISM, thus making the forecasts far more useful for practical applications. In addition, the co-variations of large scale climate variations like ENSO and IOD with the local onset/demise of the ISM rainfall raise expectations of predictability.

The arrival of the early rains in NI before the MoK is revealing. Further, its interannual variation and potential influence on the variations of the subsequent evolution of the ISM provides additional surrogates for monitoring and anticipating the ISM progression.

This local definition is necessary and appreciably more representative of the evolution of the ISM because the arrival of the first monsoon rains following the monsoon onset of Kerala (MoK) over rest of India – which is much anticipated, especially for agriculture and respite from the heat – is not uniform across the country. The proposed definition is unique in that it uses only the daily rainfall information, thus simplifying the process of the diagnosis of the evolution of ISM.

In order to avoid diagnosing false onset and demise as a result of transient weather activity unconnected to the overall ISM, we tie the diagnosis of the local onset and demise of the ISM rainfall to climatological departure from the All India averaged Rainfall (AIR) onset and demise. We achieve the diagnosis of local onset (demise) by finding local minima (maxima) in the cumulative daily anomaly rainfall curve for the grid point as close to its climatological phase difference with the corresponding AIR onset (demise). This restrictive definition of local onset (demise) however ensures avoidance of prolonged dry (wet) spells in the subsequent days.

Many previous studies have documented the climatological progression of the isochrones of onset (demise) of ISM as gradually moving from the southwest (northwest) corner of India through central and northern India and

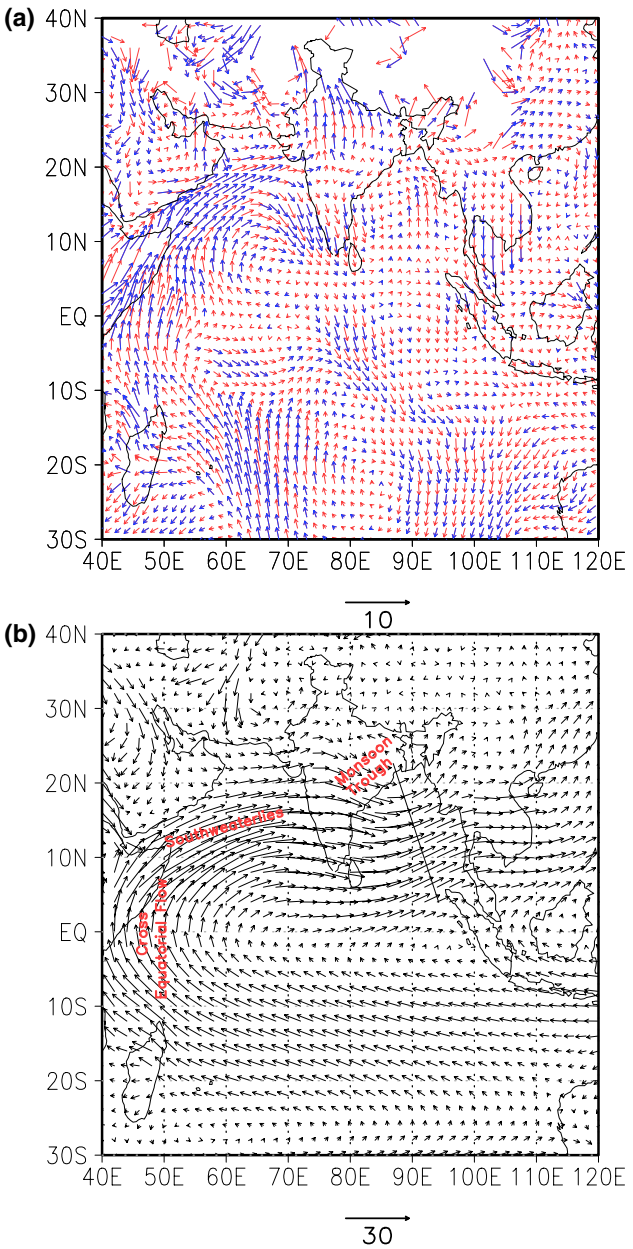


**Fig. 11** **a** The regression of the onset date of the India Summer Monsoon (ISM) over northeast India (NI) on the 850 hPa seasonal June–July–August (JJA) seasonal wind anomalies ($ms^{-1}$). The slopes have been multiplied by (−1) to indicate the anomalous flow pattern for early onset of ISM over NI. The blue arrows denote significant values at 95% confidence interval by bootstrap technique. **b** The corresponding climatological seasonal mean JJA wind flow ($ms^{-1}$) with the trough line over Bay of Bengal indicating the Monsoon trough

finally towards northwest (southeast) India, a phenomenon largely corroborated in this paper, as well. However, because of the higher granularity of our new definition (available at native grid points of the rainfall analysis), we are now able to identify the association of the anomalous onset of the ISM over Northeast India (NI) with the subsequent seasonal rainfall and length anomalies of the summer monsoon across the rest of India through its influence on the prevailing low level southwesterly flow across India. This is an important finding that illuminates the predictive potential of the variability of the early monsoon rains over NI that appears even before MoK.

**Acknowledgements** The authors thank Ms. Tracy Ippolito for her editorial assistance with the paper. The authors gratefully acknowledge the financial support given by NOAA (NA12OAR4310078) and the Earth System Science Organization, Ministry of Earth Sciences, Government of India (Grant number MM/SERP/FSU/2014/SSC-02/002) to conduct this research under Monsoon Mission. We also thank the Indian Meteorological Department for the availability of the daily rain analysis over India. The data used in this study are publicly available datasets. ERA-20C is available from https://www.ecmwf.int/en/research/climate-reanalysis/era-20c; CFSR is available from https://rda.ucar.edu/datasets/ds093.1/; and IMD rainfall analysis from http://www.imdpune.gov.in/ndc_new/ndc_index.html.

## References

Alessandri A, Borrelli A, Cherchi A, Materia S, Navarra A, Lee JY., Wang B (2015) Prediction of Indian summer monsoon onset using dynamical sub-seasonal forecasts: effects of realistic initialization of the atmosphere. Mon Weather Rev 143:778–791

Ananthakrishnan R, Acharya UR, Ramakrishnan AR, 1967 On the criteria for declaring the onset of the southwest monsoon over Kerala. IMD forecasting manual, No. IV-18.1

Ananthakrishnan R, Srinivasan V, Ramakrishnan AR, Jambunathan R (1968) Synoptic features associated with onset of southwest monsoon over Kerala, Forecast Manual, vol IV-18.2. Indian Meteorological Department, Chennai

Ashfaq M, Rastogi D, Mei R, Touma D, Leung LR (2016) Sources of errors in the simulation of South Asian summer monsoon in the CMIP5 GCMs. Clim Dyn 49:193–223

Bansod SD, Singh SV, Kriplani RH (1991) The relationship of monsoon onset with subsequent rainfall over India. Int J Climatol 11:809–817

Boos WR, Kuang Z (2010) Dominant control of the South Asian monsoon by orographic insulation versus plateau heating. Nature 463:218–222

Boos WR, Kuang Z (2013) Sensitivity of the South Asian monsoon to elevated and non-elevated heating. Sci Rep 3:1192. doi:10.1038/srep01192

Chakraborty A, Nanjundiah RS, Srinivasan J (2006) Theoretical aspects of the onset of Indian summer monsoon from perturbed orography simulations in a GCM. Ann Geophys 24:2075–2089

Efron B, Tibshirani RJ, 1993: An Introduction to the Bootstrap: Chapman and Hall, 436 p 312

Fasullo J, Webster PJ (2003) A hydrological definition of Indian monsoon onset and withdrawal. J Climate 16:3200–3211

Gadgil S, Gadgil S, 2006: The Indian Monsoon, GDP and Agriculture, Economic and Political Weekly, pp 4887–4895

Gadgil S, Guruprasad A, Srinivasan J (1992) Systematic bias in the NOAA outgoing longwave radiation dataset? J Climate 5:868–875

Gine X, Townsend RM, Vickery J, 2008: Rational expectations? Evidence from planting decisions in Semi-Arid India. Working paper No. 166, World Bank, Washington D. C., pp 41. http://

siteresources.worldbank.org/INTFR/Resources/GineTownsend-Vickery0808.pdf
Goswami BN, Sengupta D (2003) A note on the deficiency of NCEP/NCAR reanalysis surface winds over the equatorial Indian Ocean. J Geophys Res 108:3124. doi:10.1029/2002JC001497 C4
Goswami BN, Xavier PK (2005) ENSO control on the south Asian monsoon through the length of the rainy season. Geophys Res Lett 32:L18717. doi:10.1029/2005GL023216
Jain SK, Kumar V, Saharia M (2013) Analysis of rainfall and temperature trends in the northeast India. Int J Climatol 33:968–978. doi:10.1002/joc.3483
Joseph PV, Sooraj KP, Rajan CK (2006) The summer monsoon onset process over South Asia and an objective method for the date of monsoon onset over Kerala. Int J Climatol 26:1871–1893
Joseph S, Sahai AK, Abhilash S, Chattopadhyay R, Borah N, Mapes BE, Rajeevan M, Kumar A (2015) Development and evaluation of an objective criterion for the real-time prediction of Indian summer monsoon onset in a coupled model framework. J Clim 28:6234–6248
Krishnakumar V, Lau KM (1998) Possible role of symmetric instability in the onset and abrupt transition of the Asian monsoon. J Meteorol Soc Japan 76:363–383
Krishnamurti TN, Ardanay P, Ramanathan Y, Pasch R (1981) On the onset vortex of the summer monsoon. Mon Weather Rev 109:344–363. doi:10.1175/1520-0493(1981)1092.0.CO;2
Krishnamurti TN, Dubey S, Kumar V, Deepa R, Bhardwaj A (2017) Scale Interaction during an extreme rain event over South-East India. QJR Meteorol Soc Accepted Author Manuscript. doi:10.1002/qj.3016
Lindzen RS, Farrell B, Rosenthal AJ (1983) Absolute barotropic instability and monsoon depressions. J Atmos Sci 40:1178–1184
Loschnigg J, Webster PJ (2000) A coupled ocean-atmosphere system of SST regulation for the Indian Ocean. J Clim 13(19):3342–3360. doi:10.1175/1520-0442(2000)0132.0.CO;2
Lu E, Zeng X, Jiang Z, Wang Y, Zhang Q (2009) Precipitation and precipitable water: Their temporal-spatial behaviors and use in determining monsoon onsoon/retreat and monsoon regions. J Geophys Res (atmospheres) 114. doi:10.1029/2009JD012146
Lucas-Picher P, Christensen JH, Saeed F, Kumar P, Asharaf S, Ahrens B, Wiltshire AJ, Jacob D, Hagemann S, 2011: Can regional climate models represent the Indian Monsoon? J Hydrometeor 117 (5): 849{868. doi:10.1175/2011JHM1327.1
Misra V, Pantina P, Chan SC (2012) A comparative study of the Indian summer monsoon hydroclimate and its variations in three reanalyses. Climate Dyn 39:1149–1168. doi:10.1007/s00382-012-1319-y
Misra V, Bhardwaj A, Noska R (2017) Understanding the Variations of the Length and the Seasonal Rainfall Anomalies of the Indian Summer Monsoon. J Climate 30:1753–1763. doi:10.1175/JCLI-D-16-0501.1
Moron V, Robertson AW, (2014): Interannual variability of Indian summer monsoon rainfall onset date at local scale. Int J Climatol 34(4). doi:10.1002/joc.3745
Noska R, Misra V (2016) Characterizing the onset and demise of the Indian Summer Monsoon. Geophys Res Lett 43:4547–4554. doi:10.1002/2016GL068409
Pai DS, Rajeevan M (2007) Indian summer monsoon onset: variability and prediction. Indian Meteorological Department, Chennai
Pai DS, Sridhar L, Rajeevan M, Sreejith OP, Satbhai NS, Mukhopadhyay B (2014a) Development of a new high spatial resolution (0.25° × 0.25°) long period (1901–2010) daily gridded rainfall data set over India and its comparison with existing data sets over the region. Mausam 65(1):1–18
Pai DS, Sridhar L, Badwaik MR, Rajeevan M (2014b) Analysis of the daily rainfall events over India using a new long period (1901–2010) high resolution (0.25° × 0.25°) gridded rainfall data set. Climate Dyn 45(3–4). doi:10.1007/s00382-014-2307-1
Poli P, Hersbach H, Dee DP, Berrisford P, et al (2016): ERA-20C: An atmospheric reanalysis of the twentieth century. J. Climate. doi:10.1175/JCLI-D-15-0556.1
Rosenzweig M, Binswanger HP (1993) Wealth, Weather Risk and the Composition and Profitability of Agricultural Investments. Econ J 103(1):56–78
Saha S et al (2010) The NCEP Climate Forecast System Reanalysis. Bull Am Meteorol Soc 91(8):1015–1057. doi:10.1175/2010BAMS3001.1
Shah R, Mishra V (2014) Evaluation of the reanalysis products for the monsoon season droughts in India. J Hydromet 15:1575–1591
Sperber KR, Annamalai H (2014) The use of fractional accumulated precipitation for the evaluation of the annual cycle of monsoons. Climate dynamics 43(12):3219–3244
Tomas R, Webster P (1997) The role of inertial instability in determining the location and strength of near-equatorial convection. Q J R Meteorol Soc 123:1445–1482
Waliser DE, Shi Z, Lazante JR, Oort AH (1999) The Hadley circulation: assessing NCEP/NCAR reanalysis and sparse in-situ estimates. Clim Dyn 15:719–735
Walker T, Ryan J (1990) Village and Household Economics in Indias Semi-Arid Tropics. John Hopkins University Press, Baltimore
Wang B, LinHo (2002) Rainy season of the Asia-Pacific summer monsoon. J Climate 15:386–398
Wang B, Ding Q, Joseph PV (2009) Objective definition of the Indian summer monsoon onset. J Clim 22(12):3303–3316. doi:10.1175/2008JCLI2675.1
Webster PJ (2000) The coupled monsoon system. In: Wang B (ed) The Asian Monsoon. Springer, New York
Webster PJ (2013) Improve weather forecasts for the developing world. Nature. doi: 10.1038/493017a
Webster PJ, Magana VO, Palmer TN, Shukla J, Tomas RA, Yanai MU, Yasunari T (1998) Monsoons: Processes, predictability, and the prospects for prediction. J Geophys Res 103(C7):14451–14510
Wyrtki K (1973) An equatorial jet in the Indian Ocean. Science 181(4096):262–264
Yanai M, Li C, Song Z (1992) Seasonal heating of the Tibetan Plateau and its effects on the evolution of the Asian summer monsoon. J Meteorol Soc Jpn 70(1):319–351
Zeng X, Lu E (2004) Globally unified monsoon onset and retreat indexes. J Climate 17:2241–2248